Chemistry & Biology, Vol. 9, 747–755, June, 2002, ©2002 Elsevier Science Ltd. All rights reserved. PII S1074-5521(02)00153-9

Crystal Structure of a Complex between the Aminoglycoside Tobramycin and an Oligonucleotide Containing the Ribosomal Decoding A Site

Quentin Vicens and Eric Westhof[1]
Institut de Biologie Moléculaire et Cellulaire du Centre National de la Recherche Scientifique
Modélisation et Simulations des Acides Nucléiques, UPR 9002
Université Louis Pasteur
15 Rue René Descartes
67084 Strasbourg Cedex
France

Summary

Aminoglycoside antibiotics target the decoding aminoacyl site (A site) on the 16S ribosomal RNA and induce miscoding during translation. Here, we present the crystal structure, at 2.54 Å resolution, of an RNA oligonucleotide containing the A site sequence complexed to the 4,6-disubstituted 2-deoxystreptamine aminoglycoside tobramycin. The three aminosugar rings making up tobramycin interact with the deep-groove atoms directly or via water molecules and stabilize a fully bulged-out conformation of adenines A^{1492} and A^{1493}. The comparison between this structure and the one previously solved in the presence of paromomycin confirms the importance of the functional groups on the common neamine part of these two antibiotics for binding to RNA. Furthermore, the analysis of the present structure provides a molecular explanation to some of the resistance mechanisms that have spread among bacteria and rendered aminoglycoside antibiotics inefficient.

Introduction

RNA molecules constitute attractive targets for drug design because of their complex three-dimensional architectures and their essential cellular roles [1–3]. Several low-molecular-weight inhibitors are already known to bind with high affinities to different structural RNA motifs [4, 5]. Among these, aminoglycosides constitute a family of water-soluble weak bases that have similar chemical structures (Figure 1). Most of them contain a 2-deoxystreptamine part substituted at different positions by aminosugar rings, which results in polycationic derivatives at physiological pH. Whereas substitution at position 5 of the 2-deoxystreptamine ring leads to the 4,5-disubstituted subclass containing derivatives such as neomycin and paromomycin (Figure 1A), substitution at position 6 leads to the 4,6-disubstituted subclass containing antibiotics such as kanamycin, tobramycin (Figure 1B), and gentamicin (Figure 1C).

One of the main steps in protein synthesis is the recognition between messenger RNA (mRNA) and the transfer RNA (tRNA) containing the aminoacid to be incorporated. In bacteria, the recognition occurs inside the ribosome at the level of the decoding aminoacyl site (A site) on the 16S ribosomal RNA (16S rRNA) [6]. The aminoglycoside antibiotics disrupt the bacterial membrane and induce miscoding during the protein synthesis [7] by binding to the A site (Figure 2A), eventually provoking the death of the bacterial cell [8]. Previous experiments have identified the footprint of the aminoglycosides on the 16S rRNA of *Escherichia coli* [9]. Further experiments have shown that the same footprint could be observed on shorter RNA constructs containing the A site [10–13] and that aminoglycosides bind to the A site with micromolar affinity [12, 14–16]. Key binding features have been observed by NMR with a 27 nucleotide-long RNA fragment [13, 17–19] and, more recently, at 3.05 Å resolution by crystallography of the bacterial ribosomal 30S subunit complexed to paromomycin [20].

We recently solved by X-ray crystallography the structure of a complex between an RNA construct containing two bacterial A sites and two molecules of the 4,5-disubstituted paromomycin [21]. We have now solved the structure of a complex containing the aminoglycoside tobramycin. This aminoglycoside, together with gentamicin and amikacin, is one of the most commonly used in medicine because of its low cost and reliable activity [22]. This work presents the first crystal structure of the A site complexed to an aminoglycoside belonging to the 4,6-disubstituted 2-deoxystreptamine subclass. The final resolution (2.54 Å) is close enough to the resolution of the complex containing paromomycin (2.5 Å) to allow a comparison of the direct and water-bridged hydrogen bonds involving the antibiotics and the RNA. In both complexes, rings I and II, constituting the common core for the 4,5- and 4,6-disubstituted 2-deoxystreptamine aminoglycosides, bind to the A site pocket in the same way. The different recognition modes, due to the intrinsic difference in the chemical structures of the compound, help us to draw the chemical and stereochemical features important for specific binding to the A site. It is of a particular interest to notice that direct hydrogen bonds involving ring III and aminoglycoside atoms in one complex are replaced by contacts mediated via water molecules in the other complex. Therefore, the number of final contacts is roughly the same, whether ring III is attached on position 5 or 6 of ring II. These results provide an explanation for the close-to-micromolar affinity exhibited by the structurally different paromomycin and tobramycin antibiotics toward the A site. Moreover, the structure of the present complex provides molecular explanations for the resistance toward aminoglycosides that is observed in organisms having base mutations on the A site and/or enzymes chemically modifying the antibiotic.

Results and Discussion

Description of the Structure of the Complex

Crystals of complexes between oligoribonucleotides incorporating the sequence of the A site of *Escherichia coli*

[1]Correspondence: e.westhof@ibmc.u-strasbg.fr

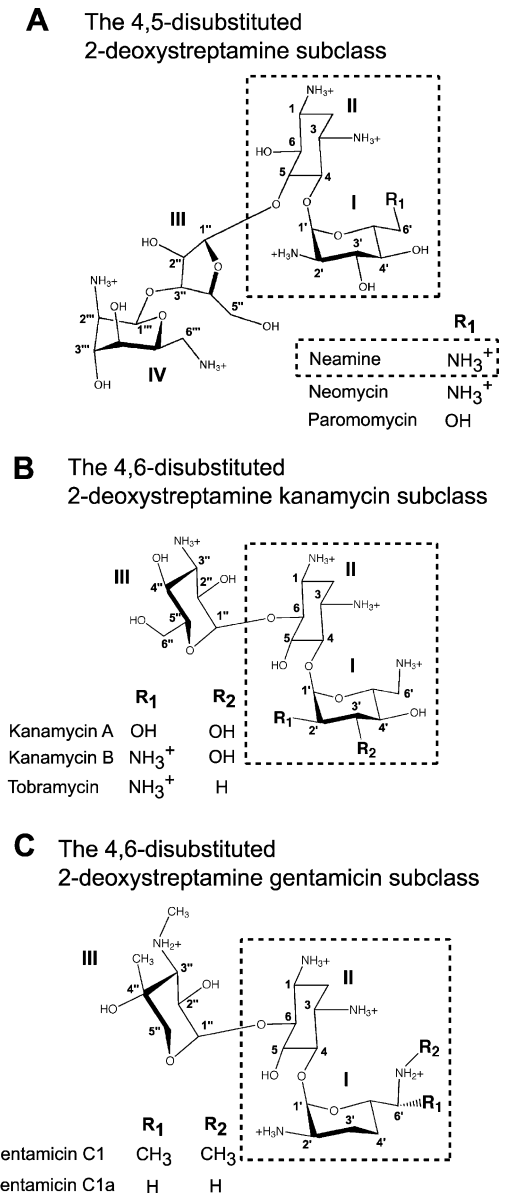

Figure 1. Chemical Structures of the Aminoglycosides

and the aminoglycoside tobramycin have been solved at 2.54 Å resolution (Table 1). Suitable crystals could be obtained only with a sequence possessing two 5′ dangling uracils, instead of the 5′ cytosines that were present in the previous structure [21]. Crystals, belonging to spacegroup $P2_1$, grow as long thin plates in similar crystallizing solutions containing tobramycin. The RNA fragment consists of a double helix incorporating the A site sequence twice (Figure 2B). Because of packing contacts similar to those observed in the paromomycin complex [21], one of the two sites (site 1) is better ordered. The two bulged adenines of site 1 make hydrogen bonds to the shallow groove of the central G=C pairs of a symmetry-related molecule. However, in site 2, the two adenines are almost perpendicular to the facing G=C and C=G pairs at the end of a symmetrical complex. The B factors observed in the latter region of the structure are high (100–120 $Å^2$), and the density is poorly defined for the atoms of the two bulging adenine bases.

Inside the A site pocket, the bulging conformation of the two adenines A^{1492} and A^{1493} is stabilized by hydrogen bonds between phosphate oxygens and exocyclic atoms of the invariant neamine part of the aminoglycosides (Figures 3A and 3B). Rings I and II, which constitute the common neamine core for the 4,5- and 4,6-disubstituted 2-deoxystreptamine aminoglycosides (Figure 1A), bind to the two A site pockets in a homologous fashion (Figures 3 and 4). Ring I intercalates in the RNA helix and thereby stacks against base G^{1491} and forms a pseudo base pair with A^{1408} (Figures 3F and 3G). The pseudo base pair between ring I and A^{1408} involves two hydrogen bonds, one between the ring oxygen and the atom N6 of A^{1408} and a second one between the donor at position 6′ on ring I (an ammonium in tobramycin and a hydroxyl in paromomycin) and the ring nitrogen N1 of A^{1408} (Figure 3F). The hydroxyl group O4′ forms a direct H bond to the anionic O2P oxygen atom of the bulging A^{1493}, and the ammonium N2′ is at the center of a tetrahedron formed by atom C2′ and three water ligands (Figure 3B). The central role of the ammonium N2′ is apparent from its coordination, although the contacts made are via water molecules. One water molecule is responsible for both bridging N2′ intramolecularly to the hydroxyl O5′ of ring II and forming a H bond to N7(G^{1491}), and it thus plays the same role as the hydroxyl O5″ of ring III in paromomycin (Figure 3B). A second water molecule forms the same bridge to O1P(A^{1493}) as in the paromomycin complex. A third water molecule forms a water bridge to O2P(A^{1492}) and thereby replaces the direct contacts formed by the hydroxyl O3′ to the same anionic phosphate oxygen in the paromomycin complex. Thus, the bulging conformation of the two adenines A^{1492} and A^{1493} is stabilized by the same number of homologous hydrogen bonds among phosphate oxygens, water molecules, and exocyclic atoms of ring I in the neamine moiety. In ring II, the ammonium N3 makes contacts to N7(G^{1494}), O2P(G^{1494}), and O1P(A^{1493}) that are identical to those seen in the paromomycin complex (Figures 3A–3E). The ammonium N1 makes an identical contact to the oxygen O4 of U^{1495} of the U^{1495}oU^{1406} pair and a homologous contact to N4(C^{1496}) mediated by one water molecule (instead of two as in the paromomycin complex) (Figures 3C and 3D). Ring II participates in two intramolecular H bonds to ring III; one involves the atoms N1 and O2″, and the second involves hydroxyl O5 and the ring oxygen O5″ (Figure 3B).

The third ring, linked to position 6 of ring II in tobramycin (instead of position 5 as in paromomycin), directly contacts the Hoogsteen sites of G^{1405} in the G^{1405}=C^{1496} pair via the hydroxyl O2″ and the ammonium N3″ (Figure 3C), as already observed by probing and structural data for other compounds of the 4,6-linked subclass [11, 19]. The other two hydroxyl groups of ring III do not make any contact to the RNA.

Comparison of the Paromomycin and Tobramycin Complexes

Both paromomycin and tobramycin bind to RNA constructs containing the A site with dissociation constants

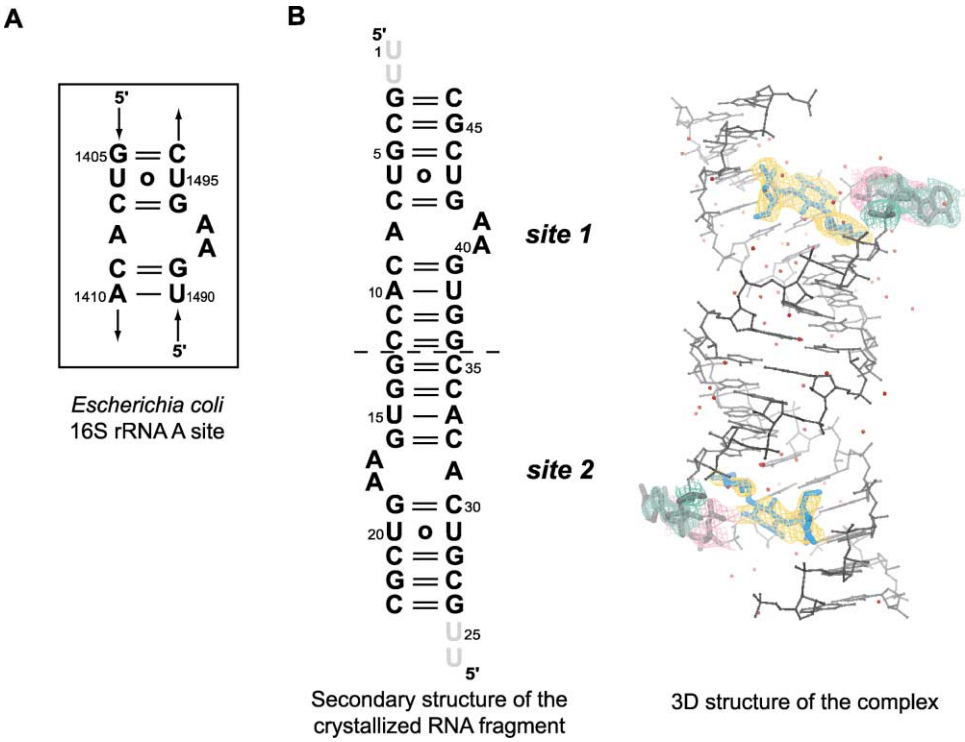

Figure 2. Secondary and Tertiary Structures of the Crystallized RNA

(A) Secondary structure of the A site of the *Escherichia coli* 16S ribosomal RNA. The standard *E. coli* numbering is specified.
(B) Secondary structure of the crystallized RNA helix. The 5′-dangling UU not observed in the density maps are shaded. The 3D structure of the crystallized complex is shown. The two tobramycin molecules (cyan) and the bulged adenines (gray) are in bold, with the 1.3σ $3F_o - 2F_c$ electron density map shown in orange for the tobramycin molecules and in green and magenta for the adenines corresponding respectively to A^{1492} and A^{1493}. The 76 water molecules are shown as red spheres.

of approximately 1.5 μM [16]. As listed in Table 2, the number of contacts in the two complexes is roughly the same (13 direct H bonds for the tobramycin complex as opposed to 15 for the paromomycin complex, a slight difference associated with the reduced number of hydroxyl groups). The main binding ligands are, as expected, the ammonium and hydroxyl groups (Table 2). The roles of the ring oxygen atoms are more subtle because these atoms participate in specific and direct H bonds but also in intramolecular H bonds within the antibiotic molecules. On the other hand, rather than making any hydrogen bond to the RNA, the ether oxygen

Table 1. Data Collection and Structure Determination

Space group	$P2_1$
Unit cell parameters (Å)	a = 46.9; b = 32.8; c = 52.0 β = 107.9°
Wavelength (Å)	0.933
Resolution range used for refinement (Å)[a]	10–2.54 (2.64–2.54)
Number of unique reflections used in refinement	4899
Redundancy	4.8
Average I/σ[a]	19.5 (9.2)
Completeness (%)[a]	95.9 (98.4)
R_{sym} (%)[ab]	5.9 (13.3)
RMS deviation for bonds (Å)	0.006
RMS deviation for angles (°)	1.0
Average B factor (Å^2)	61.4
Minimum B factor (Å^2)	17.8
Maximum B factor (Å^2)	119.1
R factor (%)[c]	21.4
R_{free} (%)[d]	26.4

[a] Values for the last shell are given between parentheses.
[b] $R_{sym} = \Sigma|I - \langle I\rangle|/\Sigma\langle I\rangle$, where I is the measured intensity of each reflection and $\langle I\rangle$ is the intensity averaged from multiple observations of symmetry-related reflections.
[c] R factor $= \Sigma||F_o| - |F_c||/\Sigma|F_o|$.
[d] R factor calculated with 7.5% of the reflections omitted from the refinement.

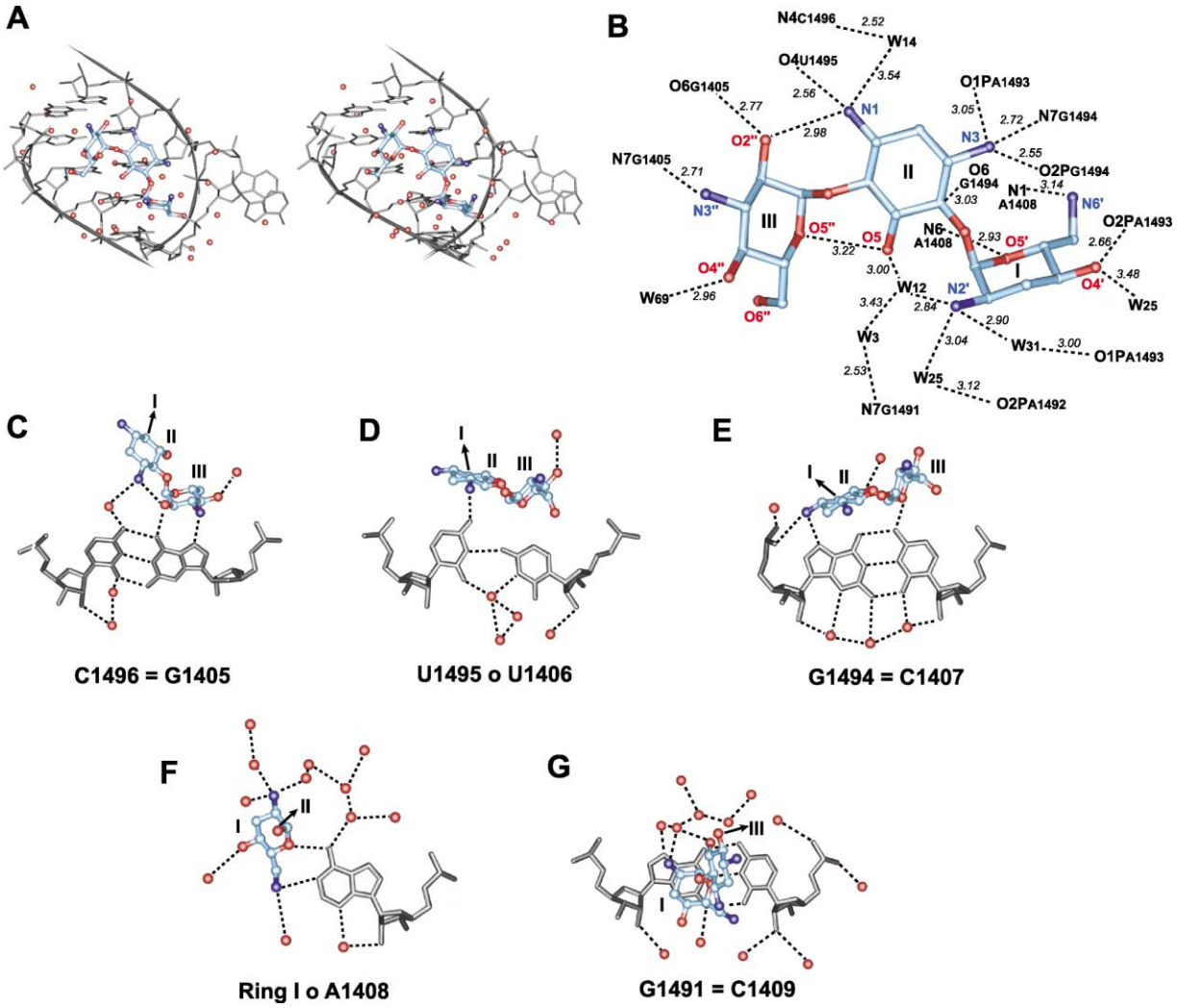

Figure 3. Close-Up of the Binding Site and Details of the Contacts

(A) Stereo view of the tobramycin in site 1. The view is toward the deep groove, with the bulged adenines on the right. Tobramycin is shown in cyan, with functional groups colored according to the atom type. Water molecules are shown as red spheres.

(B) Tobramycin close-up showing all the hydrogen bonds involving the functional groups of tobramycin. The view has the same orientation as in (A). Ring numbers and atom names are specified. The *E. coli* numbering is used for the RNA atoms, and "W" stands for a water molecule. H bonds are shown as dashed lines, with their corresponding distances in italic.

(C–G) Atomic details of the contacts involving each base pair interacting with the tobramycin inside the A site. The color code is as in (A). The name of each base pair is specified according to the *E. coli* numbering. Only a part of the tobramycin is shown at a time, with arrows pointing to the other rings.

atoms form van der Waals contacts. This is especially observed with oxygen O1′, which is in the vicinity of O1P(A^{1493}) and a water molecule (Figure 3A). However, with the oxygen atoms present as hydroxyl groups instead of ether groups (e.g., alternatively O6 and O5 on ring II of paromomycin and tobramycin), the comparison between the crystal structures containing either a 4,5-linked or a 4,6-linked aminoglycoside shows that these oxygen atoms are surrounded by water molecules (Figure 4). In the tobramycin complex, direct hydrogen bonds are observed between atoms O2″ and N3″ of ring III and the G^{1405}=C^{1496} pair (Figure 4). In the paromomycin complex, these direct contacts are replaced by water-mediated hydrogen bonds involving ring II functional groups. In the same way, the direct hydrogen bond pointing to N7(G^{1491}) in the paromomycin complex is replaced by a water-mediated hydrogen bond involving O5 of ring II and two water molecules (Figure 4). Interestingly, the binding mode of the neamine moitey can therefore be visualized. It is probable that the two rings bind in the same manner, with water-mediated hydrogen bonds replacing contacts involving the additional rings in the 4,5- and 4,6- subclasses. This would explain the lower affinity of neamine for the A site.

We can also note from the comparison between the two aminoglycoside subclasses that the intramolecular bonds play an important role in proper positioning of the rings. In the paromomycin complex, ring III is maintained in the vicinity of ring I through two intramolecular direct hydrogen bonds [21]. In the tobramycin complex,

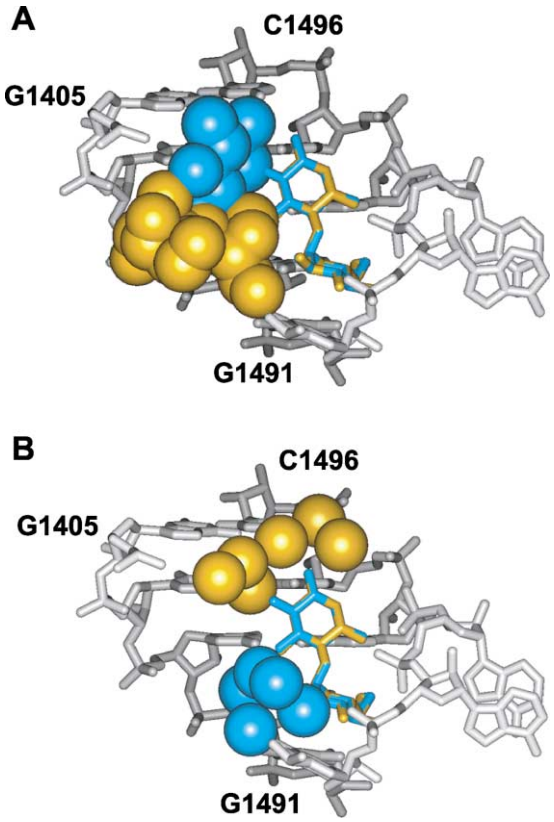

Figure 4. Superimposition of Paromomycin and Tobramycin inside the A Site in the Crystal Structures

(A) View of the A site as in Figure 3A. Paromomycin and tobramycin atoms are colored in orange and cyan, respectively. The superimposition has been done with rings I and II in the software Lsqman [46]. The common neamine part is shown as sticks, whereas the additional rings, at either position O5 (for paromomycin) or O6 (for tobramycin) of ring II, are shown as van der Waals spheres.

(B) Same view as in (A), showing only the neamine common part of the antibiotics (sticks). The water molecules replacing ring III of tobramycin in the paromomycin complex (upper part) and ring III of paromomycin in the tobramycin complex (lower part) are depicted as orange and cyan van der Waals spheres, respectively.

one water-bridged and two direct hydrogen bonds are intramolecular and seem to reinforce a conformation that enables tobramycin to bind tightly to its target (Figure 3B). Each one of these intramolecular contacts would be lost for the neamine molecule. It is noteworthy that the conformations and orientations of rings I and II of tobramycin are the same in the two completely different binding sites of RNA aptamers specific for tobramycin [23, 24]. The positions of ring III and of the exocyclic 6′ and 6″ functional groups are changed due to the different RNA environment surrounding the antibiotic, but the direct intramolecular hydrogen bonds within the antibiotic are maintained.

As concluded from several biochemical experiments [14, 25–27] and theoretical approaches [28], a key driving force in the binding of aminoglycosides to RNA is of electrostatic origin; ammonium groups of the positively charged aminoglycoside displace cations normally attracted to the negatively charged RNA. However, the number of contacts seen in these two crystalline complexes is much higher than the six hydrogen bonds seen either in the complex between neomycin and $tRNA^{Phe}$ [29] or in the modeled complex between tobramycin and polyr(I-C) [26]. It is conceivable that the latter binding modes reflect nonspecific binding of polycations to negatively charged RNA molecules [a possibility reflected by the binding constants in the upper μM range for the neomycin/$tRNA^{Phe}$ complex and in the upper mM range for the tobramycin/polyr(I-C) complex].

Comparisons with Other 4,6-Linked Aminoglycosides

Both crystal structures help understand the binding modes of the other 4,6-linked aminoglycosides (the kanamycins and the gentamicins, Figures 1B and 1C). Kanamycin B, whose affinity for the A site is very similar to that of tobramycin [16], differs from tobramycin by the presence of a hydroxyl group at the C3′ position; this hydroxyl group is also present in paromomycin. As noted above, in paromomycin, the O3′ hydroxyl forms a direct H bond with the anionic phosphate oxygen O2P(A^{1492}) and, in tobramycin, the contact with the O2P(A^{1493}) occurs via a water molecule and involves the neighboring amino group N2′ (Figure 3B). Thus, in kanamycin B, one expects a contact of the O3′ hydroxyl as in paromomycin. Kanamycin A possesses two hydroxyl groups at positions 2′ (replacing the N2′) and 3′ of ring I. Therefore, with one amino group less than tobramycin, it presents a 10-fold reduction in binding affinity [14], but the contacts to the RNA should be very similar to those formed in tobramycin (for N2′) and paromomycin (for O3′).

In the gentamicin family (Figure 1C), the amino groups N6′ of ring I and N3″ of ring III, each one forming a single contact to the RNA, are methylated (e.g., in gentamicin C1). After the structure of gentamicin antibiotics was superimposed on the crystal structure of tobramycin and the missing methyl groups were modeled, it appeared that the same direct hydrogen bonds involving ammonium groups N6′ and N3″ can occur between gentamicins and the RNA, even with gentamicin C1, which contains one methyl group on N6′ of ring I (our unpublished data). The root-mean-square deviation (rmsd) between the present X-ray structure and a single representative NMR structure of the A site complexed to the 4,6-linked gentamicin C1a [19] is 2.4 Å for all the atoms of the A site. After the superimposition of the ring atoms of the neamine part (the rmsd is 0.3 Å for the ring atoms), the other atoms constituting the A site present an rmsd of 3.6 Å between the two structures. The comparison shows that (1) in the NMR structure ring I does not intercalate into the A site pocket; (2) ring I does not form a pseudo base pair with A^{1408}; (3) adenines A^{1492} and A^{1493} do not bulge out of the helix; and (4) conserved positions in the neamine moiety do not interact with the phosphate oxygens of the bulging adenines (Figure 5). Although the pioneering NMR work [17, 19] correctly outlined the binding pocket of aminoglycosides in the A site, several conserved contacts and RNA conformations were missed. The precise knowledge of the specific contacts occurring in the binding pocket is a prerequisite not only for understanding the biological action of the antibiotic but also for the development of alternative compounds acting in an analogous fashion.

Table 2. Identical and Similar Contacts Formed by Hydrophilic Groups between the Aminoglycosides Tobramycin and Paromomycin and the RNA

Tobramycin	Paromomycin
Ammonium Groups (5)	Ammonium Groups (5)
Direct	Direct
N1...O4(U^{1495}): 2.56	**N1...O4(U^{1495}): 2.82**
N3...O1P(A^{1493}): 3.05	**N3...O1P(A^{1493}): 3.13**
N3...N7(G^{1494}): 2.72	**N3...N7(G^{1494}): 2.78**
N3...O2P(G^{1494}): 2.55	**N3...O2P(G^{1494}): 3.12**
N6′...N1(A^{1408}): 3.14	—
N3″...N7(G^{1405}): 2.71	N2‴...O2P(G^{1405}): 2.96
Water-mediated	Water-mediated
N1...W...N4(C^{1496}): 3.54/2.52	N1...W...W...N4(C^{1496}): 2.68/2.71/2.51
N2′...W...O2P(G^{1491}): 2.90/3.48	**N2′...W...O2P(G^{1491}): 3.47/3.24**
N2′...W...O1P(A^{1493}): 3.04/3.12	**N2′...W...O1P(A^{1493}): 3.27/2.89**
N2′...W...O2P(A^{1492}): 2.90/3.00	
Intramolecular	Intramolecular
N1...O2′: 2.98	N2′...O5″: 3.12
N2′...W...O5: 2.84/3.00	***N2′...O4″: 3.21***
No contact to RNA	No contact to RNA
None	N6‴
Total to RNA: 10	Total to RNA: 8
Hydroxyl Groups (5)	Hydroxyl Groups (8)
Direct	Direct
—	O3′...O2P(A^{1492}): 2.90
O4′...O2P(A^{1493}): 2.66	**O4′...O2P(A^{1493}): 2.54**
—	O6′...N1(A^{1408}): 2.53
***O2″...O6(G^{1405})**: 2.77*	O2″...N4(C^{1407}): 2.73
—	O4‴...O1P(G^{1405}): 3.77
—	***O5″...N7(G^{1491})*: 2.71**
Water-mediated	Water-mediated
O5...W...W...N7(G^{1491}): 3.00/3.43/2.53	O6...W...O4(U^{1495}): 2.62/2.98
	O6...W...O6(G^{1405}): 3.21/3.19
Intramolecular	Intramolecular
O5...O5″: 3.22	O5″...N2′: 3.12
No contact to RNA	No contact to RNA
O5	O6
O4″	O3″
O6″	—
Total to RNA: 3	Total to RNA: 8
Ring Oxygen (2)	Ring Oxygen (3)
Direct	Direct
O5′...N6(A^{1408}): 2.93	**O5′...N6(A^{1408}): 3.16**
Intramolecular	Intramolecular
O5″...O5: 3.22	O4″...N2′: 3.21
Total to RNA: 1	Total to RNA: 1
Linkage Oxygen (2)	Linkage Oxygen (3)
No contact	No contact

Identical contacts are in bold; similar contacts are in bold italics. Distances are given in Å.

Relations between the Structure of the Complex and Bacterial Resistance

Resistance in bacteria can result from different mechanisms, involving base mutations, base methylations, or enzymatic modifications of the antibiotic [30]. The role of the A1408G mutation has already been emphasized [21]. A guanine at position 1408 disfavors the binding of the aminoglycoside by presenting Watson-Crick groups not able to form the necessary direct hydrogen bonds with atoms O5′ and N6′ of ring I. Although the A1408G mutation confers resistance to aminoglycosides in eubacteria [31], it does not prevent the binding of 4,6-linked aminoglycosides to the eukaryotic A site [16], which presents a G at the equivalent position 1408, as well as an A1491 instead of a G1491 and a reversed A^{1410}-U^{1490} base pair. Antibiotics belonging to the 4,6-linked subclass might therefore bind in a slightly different manner to the eukaryotic A site in order to be active despite the base changes.

Methylation of the N7 of G^{1405} confers resistance to the 4,6-linked 2-deoxystreptamine aminoglycosides such as tobramycin but not to the 4,5-linked aminoglycosides such as paromomycin [32]. Indeed, whereas ring III of tobramycin interacts directly with N7(G^{1405}) (Figures 3A–3C), paromomycin does not reach directly to that base [21]. The mutation U1406A has also been reported to prevent the binding of aminoglycosides belonging to the 4,6-linked subclass in a selective manner

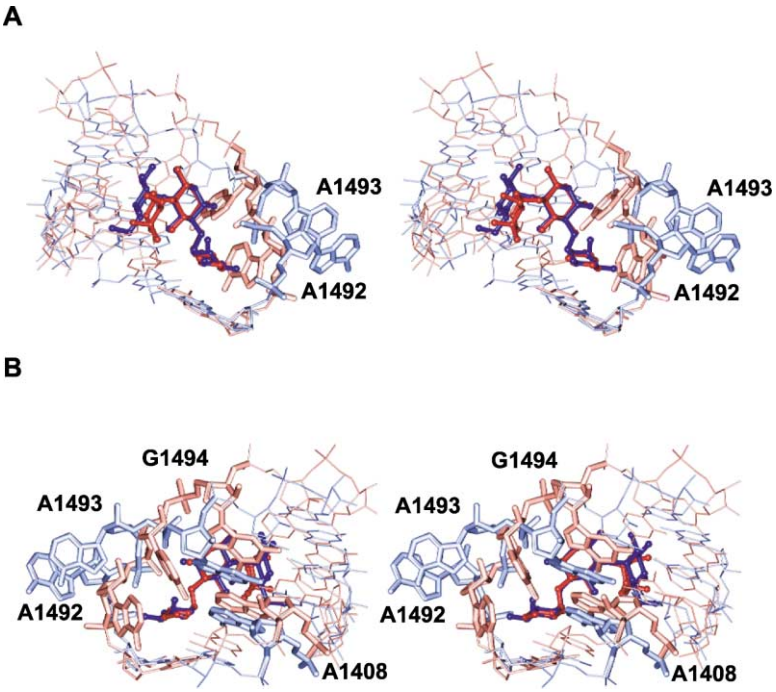

Figure 5. Superimposition of the Crystal Structure of the Tobramycin/A Site Complex and the NMR Structure of the Gentamicin C1a/A Site Complex

(A) Stereo view down the deep groove of the A site. The tobramycin/A site complex (present work) and the gentamicin C1a/A site complex (single representative structure from [19]) are colored in blue and red shades, respectively. The superimposition has been done with atoms belonging to the neamine part in the software Lsqman [46]. The adenines 1492 and 1493 are shown in bold for both complexes.

(B) Stereo view of the A site at 180° from (A). Residues A^{1408}, A^{1492}, A^{1493}, and G^{1494} are shown in bold for both complexes.

[33, 34]. In our previous structure containing paromomycin (a 4,5-linked aminoglycoside), a water molecule bridges the hydroxyl group O6 of ring II to O4 of U^{1406}. It can therefore be suspected that in the case of a U1406A mutation, a direct hydrogen bond could form between O6 of ring II and N6 of A^{1406} for 4,5-linked aminoglycosides. The involvement of O6 in the linkage with ring III in tobramycin (a 4,6-linked aminoglycoside) prevents the formation of this water-mediated hydrogen bond to O4(U^{1406}), and no other functional group of tobramycin is in a proper orientation to interact with U^{1406}. Thus, instead of preventing a direct interaction between tobramycin and the residue at position 1406, the mutation U1406A would more likely cause a steric clash between N6(A^{1406}) and ring III of tobramycin. Tobramycin and the other 4,6-linked aminoglycosides are therefore probably unable to accommodate the U1406A mutation.

Enzymatic modifications, such as adenylation and acetylation, of the aminoglycosides are mainly aimed at the neamine part functional groups (e.g., O4′, N3, and N6′) [8, 35] that are involved in critical H bonds between the aminoglycoside and the RNA. It can be inferred from the present crystal structure that adding chemical groups on these positions would prevent the formation of conserved and specific hydrogen bonds between the antibiotic and its target.

Implications for Drug Design

The comparison of the paromomycin and tobramycin complexes provides some insights for drug design. It would be indeed interesting to investigate the binding of a molecule possessing both rings in positions 5 and 6 of ring II, instead of only one. Such a strategy would maximize the number of direct H bonds to the RNA. In addition, the structure of a dimeric kanamycin A nucleotidyl transferase, which catalyzes the addition of any nucleotidyl group on position O4′ of several aminoglycosides, has been solved by X-ray crystallography while it was complexed to two kanamycin A molecules [36]. It is noteworthy that the three rings of this 4,6-disubstituted antibiotic, close in chemical structure to tobramycin, keep the same chair conformations inside the modifying enzyme, whereas their orientations to one another, possibly because of rotations around the ether linkage, are different when compared to the conformation they adopt inside the A site pocket. It could be valuable to seek the antibiotic activity of a neamine derivative having a closed ring between N2′ of ring I and O5 of ring II. Such a structure would prevent the rotations of the rings around the ether linkages. These modifications would also replace water-mediated intramolecular H bonds by covalent bonds and direct hydrogen bonds.

Significance

Small molecules binding to RNA targets have recently gained pharmaceutical interest [4, 37, 38]. Interaction of aminoglycoside antibiotics with the prokaryotic ribosomal A site is thought to be one of the sources of their bactericidal effect [8]. We have solved the structure of a complex formed by two tobramycin molecules and a construct containing two A sites. To our knowledge, this is the first X-ray crystal structure showing the interaction of a clinically used 4,6-linked aminoglycoside with the A site. Beyond the understanding of the molecular recognition and the specific resistance patterns observed in compounds belonging to this subclass, the analysis of the contacts and the comparison between this structure and the one solved with a 4,5-linked aminoglycoside paromomycin [21]

opens new directions for the development of alternative compounds with similar biological activities.

Experimental Procedures

RNA Synthesis, Purification, and Crystallization

The asymmetrical loop of the *Escherichia coli* A site (13 nucleotides) was inserted between Watson-Crick pairs in sequences designed to fold as double helices. These RNA sequences containing different lengths and ends were first checked for alternative 2D foldings with the program MFOLD [39] and then ordered from Dharmacon Research. (Boulder, CO).

Deprotected RNA oligonucleotides were purified to crystallization quality by denaturing gel electrophoresis (20% acrylamide:bisacrylamide [19:1]; 8 M urea) with TBE buffer (9 mM Tris borate [pH 8.3], 0.2 mM EDTA) at 50°C–55°C. The oligonucleotides were recovered by the "crush-and-soak" method at 4°C in 10 mM Tris (pH 7.5); 200 mM NaCl; and 0.5 mM Na EDTA for 48 hr with one buffer exchange, followed by ethanol precipitation. The pellets were washed with 95% ethanol, evaporated to dryness, and resuspended in milliQ water. Prior to crystallization experiments, tobramycin sulfate (Fluka, reference 89549) was dissolved at 28 mM in 50 mM Na cacodylate buffer (pH 6.4), and the RNA was annealed by heating at 85°C for 2 min followed by slow cooling (2 hr 30) to 37°C. Addition of tobramycin (at a final concentration of 2.2–2.3 mM) occurred at 37°C (5 min). Slow cooling then proceeded to 21°C. Hanging drops of 2 μl were made under crystallization conditions similar to the conditions that enable the formation of complexes with paromomycin [21]. One volume of crystallization solution (1.5%–4% MPD [Fluka, reference 68338]; 1%–2% glycerol; 2.2–2.3 mM tobramycin; 100–250 mM NaCl or KCl; 50 mM Na cacodylate [pH 6.4]) plus 1 volume of annealing solution (1–1.1 mM RNA; 2.2–2.3 mM tobramycin; 12.5 mM NaCl; 5 mM MgSO4; 75 mM Na cacodylate [pH 6.4]) were equilibrated against 500 μl 40% MPD. Thin crystals or spherullites were obtained after 2–3 days for most of the sequences tested, but only one sequence, containing a 5′-UU overhang, lead to plates of approximately 600 $\times$ 100 $\times$ 10 μm.

Data Collection and Processing

Crystals were equilibrated for 10 min in cryo-protecting solutions containing all the components present in the crystallization solution (but with 60%–70% MPD and 10%–20% glycerol) before being flash-cooled in liquid ethane (110 K). Data collection occurred at beamline ID14-2 of ESRF (Grenoble, France) up to a resolution of 2.54 Å (Table 1). Reflection files were indexed, scaled, and converted with Denzo [40] and the CCP4 suite [41]. The molecular replacement program AmoRe [42] found a correct solution (F_{corr} = 49.3% and R factor = 50.0%) in the resolution range 12.0–3.0 Å by using the structure of the complex containing paromomycin. The structure was refined with CNS version 1.0 [43], and the parameter and topology files for the antibiotics were calculated on the XDICT server [44]. One run of rigid-body refinement with neamine (containing only rings I and II of tobramycin) gave R and R_{free} factors of 37.1% and 37.7%, respectively. Occupancy factors were fixed to 1.0, and temperature B factors were set to 30.0 Å^2 and then refined isotropically on a 6–2.5 Å resolution range by torsion simulated annealing refinement (starting at 2500 K and cooling slowly at 50 K/min) and manual rebuilding in the calculated σA-weighted $3F_o - 2F_c$ and $F_o - F_c$ electron density maps.

The maps did not show any density for the 5′-UU overhang but showed clearly the density for the tobramycin in the two sites. However, as already observed in the structure with paromomycin, site 2 is less well defined than site 1. The density of the bulged adenines A17 and A18 is poorly defined, except for the phosphates and some of the sugar atoms. The algorithm of the software Buster [45] managed to calculate a better-defined density for the two bulged adenines, although the density of the base A18 remains poor. The refinement was pursued (in CNS) by the energy minimization protocol (8–2.54 Å/four cycles of 200 steps). After rearrangements of the substitutive groups on the antibiotic and careful addition of water molecules, the duplex was refined to reach a final R = 21.4% and an R_{free} = 26.4%. The final model contains 900 RNA atoms, 64 tobramycin atoms, and 76 water molecules.

Acknowledgments

We are grateful to Vincent Mikol and Jean-Pierre Guilloteau at Aventis for encouragement and support. We gratefully thank Philippe Dumas, Eric Ennifar, Magali Mathieu, Benoît Masquida, and the people of beamline ID14-2 at ESRF (Grenoble, France) for their help with the data collection and refinement. We thank Pascal Auffinger and Frank Walter for helpful discussions. Q.V. is supported by a Bourse Docteur-Ingénieur from the Centre National de la Recherche Scientifique/Aventis.

Received: March 6, 2002
Revised: April 10, 2002
Accepted: April 15, 2002

References

1. Hermann, T., and Westhof, E. (1998). RNA as a drug target: chemical, modelling, and evolutionary tools. Curr. Opin. Biotechnol. *9*, 66–73.
2. Ban, N., Nissen, P., Hansen, J., Moore, P.B., and Steitz, T.A. (2000). The complete atomic structure of the large ribosomal subunit at 2.4 Å resolution. Science *289*, 905–920.
3. Sucheck, S.J., and Wong, C.H. (2000). RNA as a target for small molecules. Curr. Opin. Chem. Biol. *4*, 678–686.
4. Hermann, T. (2000). Strategies for the design of drugs targeting RNA and RNA-protein complexes. Angew. Chem. Int. Ed. *39*, 1890–1905.
5. Wilson, W.D., and Li, K. (2000). Targeting RNA with small molecules. Curr. Med. Chem. *7*, 73–98.
6. Ramakrishnan, V., and Moore, P.B. (2001). Atomic structures at last: the ribosome in 2000. Curr. Opin. Struct. Biol. *11*, 144–154.
7. Davies, J., and Davis, B.D. (1968). Misreading of ribonucleic acid code words induced by aminoglycoside antibiotics. J. Biol. Chem. *243*, 3312–3316.
8. Wright, G.D., Berghuis, A.M., and Mobashery, S. (1998). Aminoglycoside antibiotics. Structures, functions, and resistance. In Resolving the Antibiotic Paradox: Progress in Understanding Drug Resistance and Development of New Antibiotics. B.P. Rosen and S. Mobashery, eds. (New York: Plenum Press), pp. 27–69.
9. Moazed, D., and Noller, H.F. (1987). Interaction of antibiotics with functional sites in 16S ribosomal RNA. Nature *327*, 389–394.
10. Purohit, P., and Stern, S. (1994). Interactions of a small RNA with antibiotics and RNA ligands of the 30S subunit. Nature *370*, 659–662.
11. Miyaguchi, H., Narita, H., Sakamoto, K., and Yokoyama, S. (1996). An antibiotic-binding motif of an RNA fragment derived from the A-site related region of *Escherichia coli* 16S RNA. Nucleic Acid Res. *24*, 3700–3706.
12. Recht, M.I., Fourmy, D., Blanchard, S.C., Dahlquist, K.D., and Puglisi, J.D. (1996). RNA sequence determinants for aminoglycoside binding to an A-site rRNA model oligonucleotide. J. Mol. Biol. *262*, 421–436.
13. Blanchard, S.C., Fourmy, D., Eason, R.G., and Puglisi, J.D. (1998). rRNA chemical groups required for aminoglycoside binding. Biochemistry *37*, 7716–7724.
14. Wong, C.-H., Hendrix, M., Priestley, E.S., and Greenberg, W.A. (1998). Specificity of aminoglycoside antibiotics for the A-site of the decoding region of ribosomal RNA. Chem. Biol. *5*, 397–406.
15. Griffey, R.H., Hofstadler, S.A., Sannes-Lowery, K.A., Ecker, D.J., and Crooke, S.T. (1999). Determinants of aminoglycoside-binding specifity for rRNA by using mass spectrometry. Proc. Natl. Acad. Sci. USA *96*, 10129–10133.
16. Hyun Ryu, D., and Rando, R.R. (2001). Aminoglycoside binding to human and bacterial A-Site rRNA decoding region constructs. Bioorg. Med. Chem. *9*, 2601–2608.
17. Fourmy, D., Recht, M.I., Blanchard, S.C., and Puglisi, J.D. (1996). Structure of the A-site of *Escherichia coli* 16S ribosomal RNA complexed with an aminoglycoside antibiotic. Science *274*, 1367–1371.
18. Fourmy, D., Recht, M.I., and Puglisi, J.D. (1998). Binding of

neomycin-class aminoglycoside antibiotics to the A-site of 16 S rRNA. J. Mol. Biol. *277*, 347–362.
19. Yoshizawa, S., Fourmy, D., and Puglisi, J.D. (1998). Structural origins of gentamicin antibiotic action. EMBO J. *17*, 6437–6448.
20. Carter, A.P., Clemons, W.M., Brodersen, D.E., Morgan-Warren, R.J., Wimberly, B.T., and Ramakrishnan, V. (2000). Functional insights from the structure of the 30S ribosomal subunit and its interactions with antibiotics. Nature *407*, 340–348.
21. Vicens, Q., and Westhof, E. (2001). Crystal structure of paromomycin docked into the eubacterial ribosomal decoding A site. Structure *9*, 647–658.
22. Gonzalez, L.S.I., and Spencer, J.P. (1998). Aminoglycosides: a practical review. American Family Physician, www.aafp.org/afp/981115ap/gonzalez.html.
23. Jiang, L., Suri, A.K., Fiala, R., and Patel, D.J. (1997). Saccharide-RNA recognition in an aminoglycoside antibiotic-RNA aptamer complex. Chem. Biol. *4*, 35–50.
24. Jiang, L.C., and Patel, D.J. (1998). Solution structure of the tobramycin-RNA aptamer complex. Nat. Struct. Biol. *5*, 769–774.
25. Wang, H., and Tor, Y. (1998). RNA-aminoglycoside interactions: design, synthesis and binding of "amino-aminoglycosides" to RNA. Angew. Chem. Int. Ed. *37*, 109–111.
26. Jin, E., Katritch, V., Olson, W.K., Kharatisvili, M., Abagyan, R., and Pilch, D.S. (2000). Aminoglycoside binding in the major groove of duplex RNA: the thermodynamic and electrotatic forces that govern recognition. J. Mol. Biol. *298*, 95–110.
27. Wang, H., and Tor, Y. (1997). Electrostatic interactions in RNA aminoglycosides binding. J. Am. Chem. Soc. *119*, 8734–8735.
28. Hermann, T., and Westhof, E. (1999). Docking of cationic antibiotics to negatively charged pockets in RNA folds. J. Med. Chem. *42*, 1250–1261.
29. Mikkelsen, N.E., Johansson, K., Virtanen, A., and Kirsebom, L.A. (2001). Aminoglycoside binding displaces a divalent metal ion in a tRNA-neomycin B complex. Nat. Struct. Biol. *8*, 510–514.
30. Walsh, C. (2000). Molecular mechanisms that confer antibacterial drug resistance. Nature *406*, 775–781.
31. Recht, M.I., Douthwaite, S., and Puglisi, J.D. (1999). Basis for prokaryotic specificity of action of aminoglycoside antibiotics. EMBO J. *18*, 3133–3138.
32. Beauclerk, A.A., and Cundliffe, E. (1987). Sites of action of two ribosomal RNA methylases responsible for resistance to aminoglycosides. J. Mol. Biol. *193*, 661–671.
33. Taniguchi, H., Chang, B., Abe, C., Nikaido, Y., Mizuguchi, Y., and Yoshida, S.I. (1997). Molecular analysis of kanamycin and viomycin resistance in *Mycobacterium smegmatis* by use of the conjugation system. J. Bacteriol. *179*, 4795–4801.
34. Recht, M.I., and Puglisi, J.D. (2001). Aminoglycoside resistance with homogeneous and heterogeneous populations of antibiotic-resistant ribosomes. Antimicrob. Agents Chemother. *45*, 2414–2419.
35. Azucena, E., and Mobashery, S. (2001). Aminoglycoside-modifying enzymes: mechanisms of catalytic processes and inhibition. Drug. Resist. Updat. *4*, 106–117.
36. Pedersen, L.C., Benning, M.M., and Holden, H.M. (1995). Structural investigation of the antibiotic and ATP-binding sites in kanamycin nucleotidyltransferase. Biochemistry *34*, 13305–13311.
37. Xavier, K.A., Eder, P.S., and Giordano, T. (2000). RNA as a drug target: methods for biophysical characterization and screening. Trends Biotechnol. *18*, 349–356.
38. Gallego, J., and Varani, G. (2001). Targeting RNA with small-molecule drugs: therapeutic promise and chemical challenges. Acc. Chem. Res. *34*, 836–843.
39. Mathews, D.H., Sabina, J., Zuker, M., and Turner, D.H. (1999). Expanded sequence dependence of thermodynamic parameters improves prediction of RNA secondary structure. J. Mol. Biol. *288*, 911–940.
40. Otwinowski, Z., and Minor, W. (1996). Processing of X-Ray diffraction data collected in oscillation mode. In Methods Enzymol. C.W. Carter, Jr. and R.M. Sweet, eds. (New York: Academic Press).
41. CCP4 (Collaborative Computational Project 4) (1994). The CCP4 suite: programs for protein crystallography. Acta Crystallogr. D *50*, 760–763.
42. Navaza, J. (1994). AMoRe: an automated package for molecular replacement. Acta Crystallogr. A *50*, 157–163.
43. Brünger, A.T., Adams, P.D., Clore, G.M., DeLano, W.L., Gros, P., Grosse-Kunstleve, R.W., Jiang, J.S., Kuszewski, J., Nilges, M., Pannu, N.S., et al. (1998). Crystallography & NMR system: a new software suite for macromolecular structure determination. Acta Crystallogr. D *54*, 905–921.
44. Kleywegt, G.J., and Jones, T.A. (1997). Model-building and refinement practice. In Methods Enzymol. C.W. Carter, Jr and R.M. Sweet, eds. (New York: Academic Press), pp. 208–230.
45. Bricogne, G. (1993). Direct phase determination by entropy maximization and likelihood ranking: status report and perspectives. Acta Crystallogr. D *49*, 37–60.
46. Kleywegt, G.J. (1996). Use of non-crystallographic symmetry in protein structure refinement. Acta Crystallogr. D *52*, 842–857.

Accession Numbers

The structure has been entered in the Protein Data Bank with ID code 1LC4.